Multiinput DC–DC converters in renewable energy applications – An overview

CrossMark

Zubair Rehman *, Ibrahim Al-Bahadly, Subhas Mukhopadhyay

School of Engineering and Advanced Technology, Massey University, Palmerston North, New Zealand

ARTICLE INFO

ABSTRACT

Power electronics DC–DC converters are being widely used in various applications like hybrid energy systems, hybrid vehicles, aerospace, satellite applications and portable electronics devices. In the recent past, a lot of research and development has been carried out to enhance the reliability, efficiency, modularity and cost effectiveness of these converters. A number of new topologies have been proposed and new characteristics of power conversion have been defined. DC–DC converters have made a successful transition from single input–single output to multiinput–multioutput converters. These converters are now able to interface different level inputs and combine their advantages to feed the different level of outputs. Research is continued to bring down the cost and reduce the number of components while keeping the continuous improvement in the areas like reliability and efficiency of the overall system. The study of different multiinput DC–DC converter topologies suggests that there is no single topology which can handle the entire goals of cost, reliability, flexibility, efficiency and modularity single handed. This paper presents some of the recent trends in the development of multiinput and multioutput DC–DC converters. Methods to synthesize multiinput converters, their operational principles, merits and demerits are studied.

© 2014 Elsevier Ltd. All rights reserved.

Contents

* Correspondence to: School of Engineering and Advanced Technology, Massey, University, Turitea Campus, Palmerston North, New Zealand. Tel.: +64 6 3569099 84147; fax: +64 6 3569099 2259.
E-mail address: z.rehman1@massey.ac.nz (Z. Rehman).

1. Introduction

Recent developments in renewable energy based power systems, hybrid vehicles, aerospace systems, renewable energy based smart grids and hand held portable devices have brought challenges to design new DC–DC power conversion systems. This new systems will be composed of several input energy sources, integrated through a multiinput power electronics converters that could accommodate a variety of input sources and combine their advantages to deliver a controlled output for diversified applications. Two structures for DC–DC conversion have been reported in the literature. In the conventional structure, as shown in Fig. 1, multiple sources are combined at a common DC bus and separate DC–DC conversion stages are employed for individual sources and converters are controlled independently [1,2]. In some cases a communication bus is also added for exchange of information between sources. This structure of DC–DC conversion is used in grid connected and standalone hybrid energy systems [3,4]. As this system involves power conversion at multiple stages and communication devices are sometimes required, therefore the resulting cost of the converter is on higher side. The independent control of several converters also makes the system complex.

To overcome these disadvantages, a multiport structure is adopted as shown in Fig. 2. In this system, the whole structure is treated as a single power converter, which combines multiple sources and the power regulation is performed by controllers. Due to their simple structure, minimum number of conversion stages and less devices, these multiport power electronics converters have been presented for a number of applications like hybrid energy systems [5–7] hybrid vehicles [8,9] satellite/aerospace applications and uninterrupted power supplies [10,11]. These are further divided into two categories: (a) isolated and (b) nonisolated converters. Isolated converters [12,13] are used to isolate the low voltage DC side from high voltage side to avoid shock hazard, to achieve high voltage conversion, for voltage matching and to avoid large current/voltage rating semiconductor devices. High frequency transformers are used for this purpose. But the disadvantage of this system is that it needs to accommodate a transformer core which makes it bulky and in terms increases the cost. The non-isolated converters on the other hand are simple in structure and are used where the galvanic insulation between source and load is not required. The advantage of this topology is low cost due to less number of components and it can
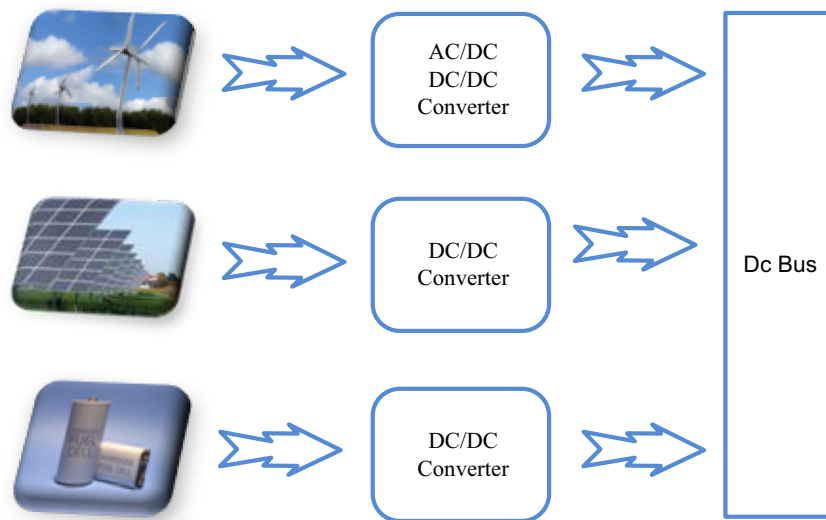

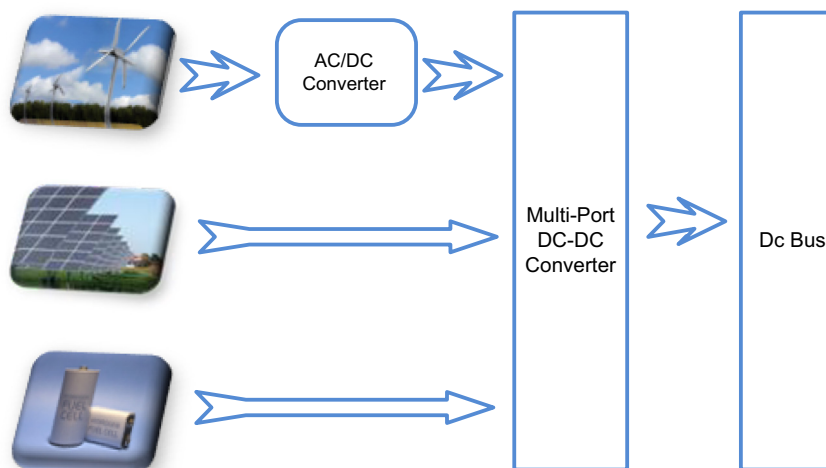**Fig. 1.** Conventional single-port structure.

Fig. 2. Multiport DC–DC converter structure.

achieve high power density. Non-isolated converters can match the input impedance of source and the output impedance of load but theses converters cannot achieve a high voltage conversion ratio.

In this paper some recent development trends in the field of multi-input DC–DC converter topologies for renewable energy system applications are studied and presented. Operational principle, advantages and disadvantages of multiinput DC–DC converters are discussed. Rest of the paper is divided in the following sections:

Section 2 presents multiinput non-isolated DC–DC converters.
Section 3 presents the comparison of non-isolated converters.
Section 4 presents multiinput isolated DC–DC converters.
Section 5 presents challenges and future work.
Conclusions are drawn in Section 6.

2. Multiinput non-isolated DC–DC converters

2.1. Dual input–single output DC–DC converters

Dual input–single output DC–DC converters are proposed and analyzed for a high and a low voltage source in [14–16] as shown in Fig. 3. This converter is a combination of the buck–boost and the buck converter. Four modes of operation are defined which are based on availability of input voltage sources and conduction state of their respective switches (S_1 and S_2). Low voltage source (V_{low}) is considered as the primary input source to provide the base load whereas the high voltage source (V_{hi}) caters the additional load demand. Input voltage sources (individually and simultaneously) charge the inductor during the ON state of their respective switches. When switches are ON, the diodes are reverse biased and when the switches are OFF, diodes (D_1 and D_2) provide the path for discharge of inductor current. Typical waveforms of inductor voltage (V_L), inductor current (I_L), and gate signals (V_{ghi} and V_{glow}) are shown in Fig. 4. If one of the voltage sources is not available, other source will provide energy to the load.

The input–output voltage relationship is derived from the volt–second balance analysis of the inductor in steady state conditions. The output voltage (V_o) can be expressed as

$$V_o = \frac{d_1}{1-d_2}V_{hi} + \frac{d_2}{1-d_2}V_{low} \qquad (1)$$

where d_1 and d_2 are the duty ratios of switches S_1 and S_2 respectively. To minimize the switching loss and to improve the overall efficiency, a passive lossless switching is added in the
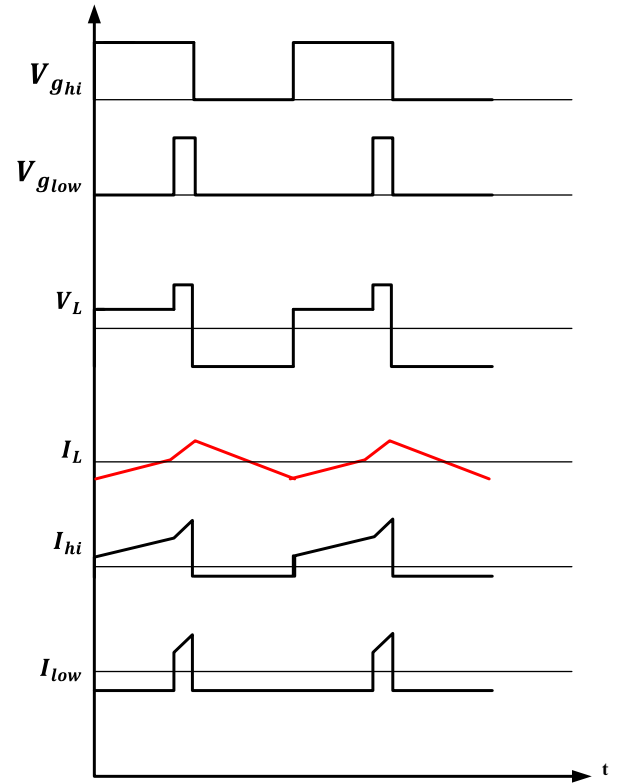

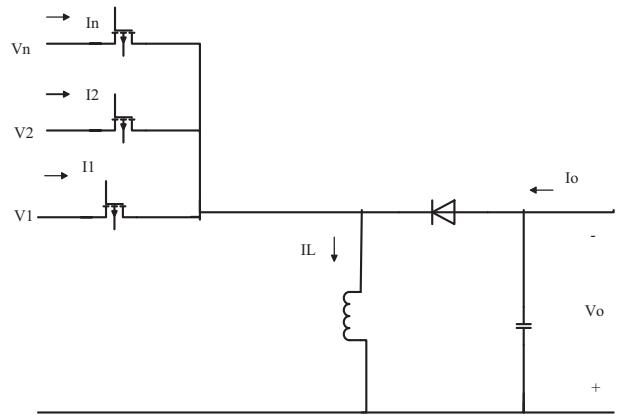**Fig. 4.** Typical current and voltage waveforms of double input converter.

Fig. 5. Unidirectional multiinput buck–boost converter.

circuit. Control scheme of the proposed converter along with detailed analytical and experimental results are presented.

A topology with n-numbered inputs based on buck–boost converter is proposed in [17] as shown in Fig. 5. This converter has reduced the circuit components but its drawback is negative reference output which can be reversed by using a transformer, which adds to the cost and size of the topology. The converter operates in one direction and another converter is required for bidirectional operation. Another drawback of this topology is that only one source can deliver the power at a time. These drawbacks are removed by a bidirectional multiinput DC–DC converter topology, introduced in [18] as shown in Fig. 6. In addition to the advantages described in [17], this topology provides positive output voltage without any additional transformer. It can also operate in bidirectional mode without the requirement of any additional converter. It operates in three modes i.e. buck, boost,

Fig. 3. Double input buck–buck boost converter.

Fig. 6. Bidirectional multiinput converter.

Fig. 7. Dual input buck–buck converter.
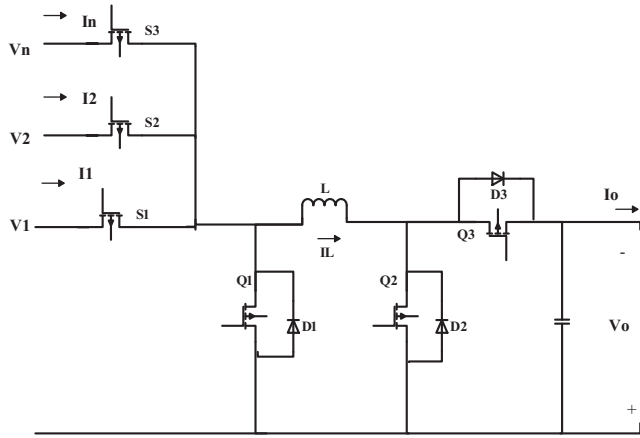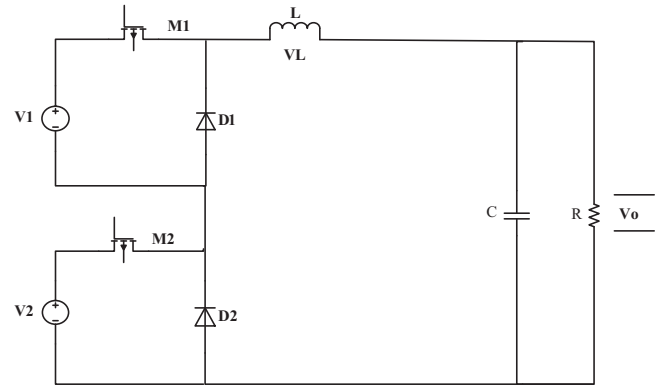
and buck–boost. But the number of devices has increased which increases the conduction losses and also makes the converter costly. The conduction losses of switches in dual power state can be greatly reduced in the boost converter proposed in [19]. In this topology bidirectional operation is achieved by applying less number of controllable switches. However the reverse recovery current in output diode reduces the overall efficiency of the converter. The issue is addressed in a Zero Voltage Switching multi-input converter investigated in [20]. This converter utilizes current sources at input. Conduction losses of the switches are reduced due to series of connected input cells and Pulse Width Modulated (PWM) signals in the dual-power-supply state. An auxiliary circuit is added in the discontinuous conduction mode (DCM) to achieve turn-on zero voltage switching of all switches. Reverse-recovery current of the output diode in boost converter is removed by an auxiliary inductor connected in series with Schottky diode. In this converter, two power sources with different voltage levels are converted to a single stable DC output. Another high-efficiency ZVS dual-input converter is investigated and experimentally tested in [21], utilizing zero current switching turn OFF of all active switches by a modified auxiliary cell proposed in [22]. The reverse-recovery currents of the diodes and the switching losses of the switches are reduced. The overall efficiency of more than 95% has been achieved and this converter can be used for high voltage applications. However this converter can induce electromagnetic interference (EMI) problems if used for non-isolated photo voltaic (PV) applications.

Two topologies like integrated buck–buck (Fig. 7) and integrated buck boost–buck boost (Fig. 9) are presented in [23,24]. The former topology is able to deliver the output power individually and simultaneously with both the sources whereas in the later topology voltage sources are unable to feed the load simultaneously. The following four modes of operation are defined for buck–buck converter topology (Fig. 7) depending on the condition of switches. Typical current and voltage waveforms are shown in Fig. 8.

Mode I [M_1: ON/M_2: OFF]: As M_1 conducts in this mode therefore diode D_1 is reverse biased whereas diode D_2 provides a bypass path for inductor current I_L. Voltage source V_1 provides power to inductor and the load.
Mode II [M_1: ON/M_2: ON] both the switches are conducting and both the diodes are blocking. Both the voltage sources connected in series and both energize inductor and provide energy demand for load.
Mode III [M_1: OFF/M_2: ON]: In this mode switch M_2 and diode D_1 are in the state of conduction while diode D_2 is OFF. Voltage
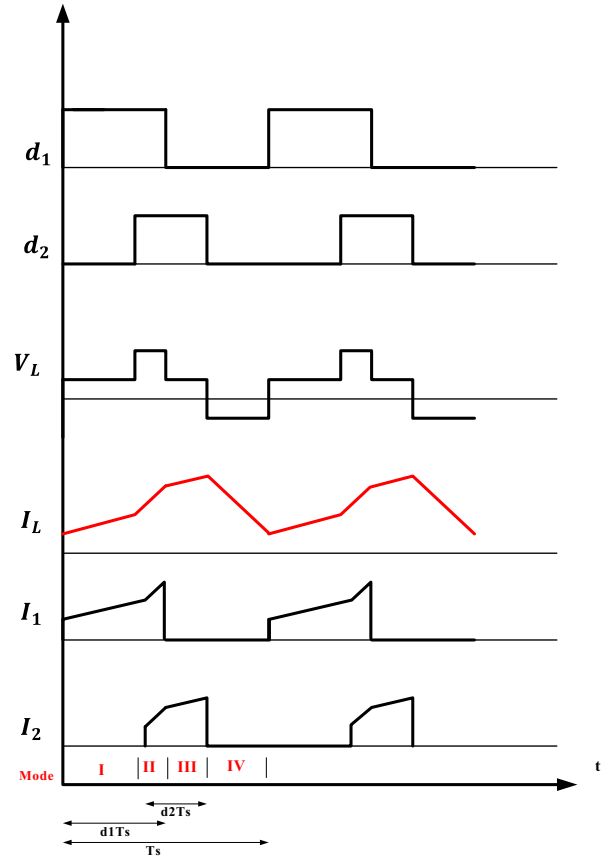
Fig. 8. Typical waveforms of dual input buck–buck converter.

source V_2 is responsible to energize inductor and powers up the load.
Mode IV [M_1: OFF/M_2: OFF] As both the switches are OFF therefore the diodes D_1 and D_2 provide the path for flow of current and the inductor discharges to release stored energy to the load. If a single source operates, the power conversion operation is same as in the conventional buck converter. By applying volt–second balance theorem, the input–output voltage relation can be obtained and is given by

$$V_o = V_1 d_1 + V_2 d_2 \tag{2}$$

where d_1 and d_2 are the duty ratios of switches S_1 and S_2, respectively and V_o is the output voltage.

In the topologies reported from [12–24], the method of developing dual or multiinput converters from single input converter has not been explained. This method is explained in detail in [25,26]. In this work, the concept of the pulsating voltage-source cell (PVSC) and the pulsating current-source cell (PCSC) has been introduced. These pulsating source cells (PSCs) are extracted from the six basic non-isolated converters like buck, boost, buck–boost, Cuk, Zeta, and SEPIC converters. Two families of multiinput converters (MICs) have been generated by inserting these PSCs into the six basic non-isolated converters. The input sources of the generated non-isolated MICs can transfer energy to the load individually or simultaneously. However the topologies with time-multiplexing control scheme are not considered in this approach. Feasible topologies of multiinput DC–DC converters based on some conditions, assumptions and restrictions are identified and several multiinput converters are derived with time multiplexing control scheme [27]. Multiinput converters (MICs) are also synthesized by using six basic pulse width modulated DC–DC converters by a systematic method [28]. Two types of MICs are considered one which allows only single source to transfer power to output load at a time, and the other allows both the input sources to deliver energy to output load either individually or simultaneously. The basic cells for constructing DC–DC converters have been discussed first and then basic pulsating voltage source cells and, basic pulsating current source cells, and hybrid pulsating source cells (PSCs) are proposed and the rules for connecting PSCs are defined and finally two families of MICs are developed.

Muntean et al. [29] proposed a hybrid multi-input DC–DC converter for high step-down conversion voltage ratio. In this topology, the output voltage can vary in a wider range. The proposed dual input hybrid DC–DC converters are obtained using hybrid and classical buck structures. The output/input relationship is given as

$$V_O = \frac{2D_1 - D_2}{2 - D_2}V_1 + \frac{D_2}{2 - D_2}V_2 \quad \text{for } D_1 > D_2 \quad (3)$$

$$V_O = \frac{D_1}{2 - D_2}V_1 + \frac{D_2}{2 - D_2}V_2 \quad \text{for } D_1 \leq D_2 \quad (4)$$

where V_O is the output voltage, V_1 and V_2 are the input voltages for sources 1 and 2 and D_1 and D_2 are the duty ratios of the switches. The output voltage in this topology is reduced by a factor $(2 - D_2)$, which is lower than that of the normal buck converter. Similar approach has been adopted in [30,31] using a multiinput hybrid buck LC converter for a standalone small hybrid wind turbine and PV with battery storage system. Analysis, simulations, and experimental results show that this topology has the advantage of a high input to output voltage conversion ratio without using a transformer, which facilitates the connection of a low voltage battery to the renewable sources at a higher voltage. Three operating modes have been discussed and the results show that the system operation is stable in each operating mode. However efficiency of the converter has not been taken into account in the experiments.

Kumaravel and Ashok [32] proposed a multiinput power conditioner with two input and one output DC–DC boost converter for a hybrid electric system. The proposed system overcomes capacitor voltage imbalance problem associated with single sourced converters. This converter has the advantages like lower voltage stress on the power switch employed in DC–DC converter, less switching loss of the switch, regulated output and can deliver reliable output power. Simulation has been carried out using the real weather data. The obtained results show that the topology can be highly beneficial in renewable energy applications. A multi-input DC–DC converter is proposed with the integration of Cuk and SEPIC converters in [1]. The advantages of this topology are
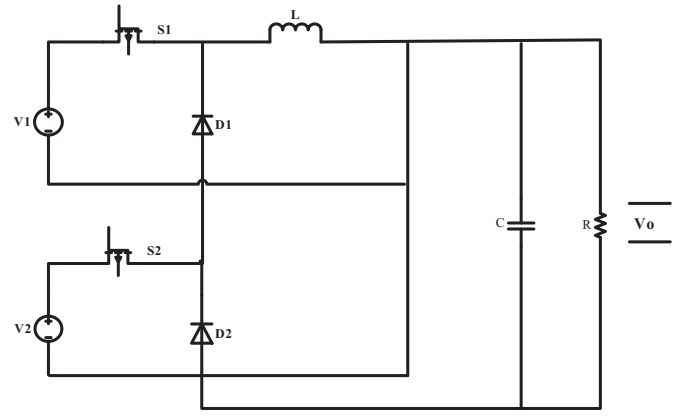

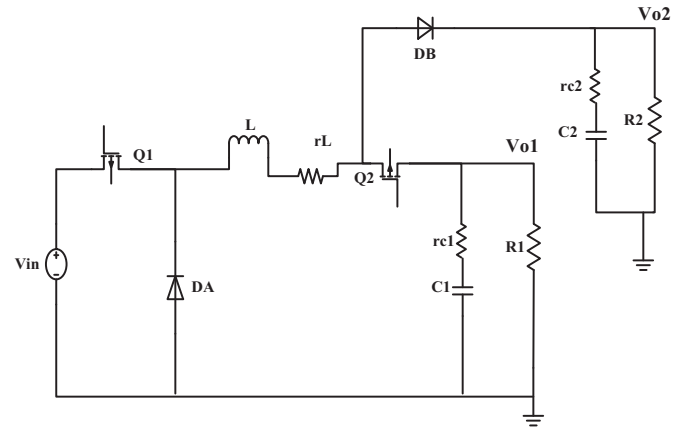**Fig. 9.** Dual input buck boost–buck boost converter.

Fig. 10. Single input–dual output buck converter.

there is no need of separate input filters, can support step up/down operations for each renewable energy source, can ensure maximum power point tracking (MPPT) for each source and supports individual and simultaneous operation modes.

2.2. Single input–dual output DC–DC converters

Single input–dual output converters (SIDO) are being used in portable applications like digital cameras, cellular phones, hand held devices, MP3 players, etc. [33]. Several SIDO converters have been reported in the literature. Fig. 10 shows a circuit diagram of a SIDO converter. Q_1 and Q_2 are the controlled switches, V_{in} is the input voltage, V_{01} and V_{02} are the two output voltages, D_A and D_B are diodes. Three classes are investigated in continuous conduction mode depending on input–output voltages, duty cycles d_1 and d_2 of respective switches [34,35].

Class-1: $d_1 > d_2$
In this case, during time period t_1, both the switches are turned ON. The inductor is charged with the current $I_L = (V_{in} - V_{o1})/L$ and the diode D_B is reverse biased due to the fact $V_{o2} > V_{o1}$. During the next time period t_2, Q_1 is still on but Q_2 is turned OFF, the inductor current ramps up with the slope $(V_{in} - V_{o2})/L$ and flows through diode D_B to the output V_{o2}. During the time period t_3 when both Q_1 and Q_2 are off, the inductor current I_L flows through both the diodes D_A and D_B and discharges through V_{o2}. In this class of operation, the inductor is charged through two periods and is discharged to output load R_2 in the last period.
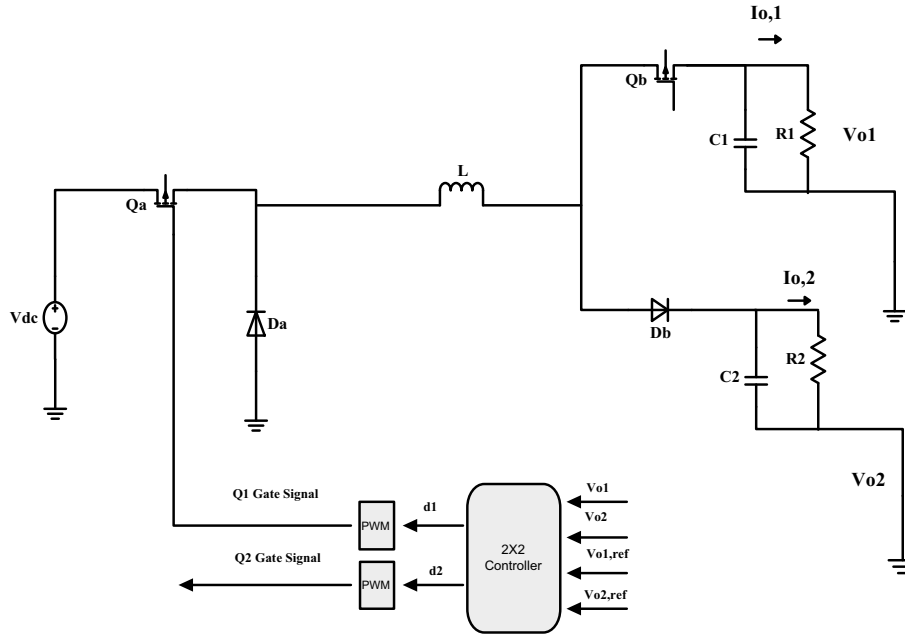
Fig. 11. Single inductor dual output converter with multivariable control.

Class-2: $d_1 = d_2$

In this case both the switches are turned ON. The inductor is charged with the current $I_L = (V_{in} - V_{o1})/L$ and the diode D_B is reverse biased due to the fact $V_{o2} > V_{o1}$. In the next time duration, when both Q_1 and Q_2 are turned OFF, the inductor current flows through both diodes and discharges to output V_{o2}. In this class of operation, the inductor is charged through one period and is discharged to output voltage in the last period.

Class-3: $d_1 < d_2$

Both the switches are ON during the time period t_1. The inductor is charged with the current $I_L = (V_{in} - V_{o1})/L$ and the diode D_B is reverse biased due to the fact $V_{o2} > V_{o1}$. During the time period t_2, switch Q_2 is still on but Q_1 is turned OFF. The inductor current flows down to V_{o1} with the slope of V_{o1}/L through diode D_A. During the time period t_3, both Q_1 and Q_2 are off, the inductor current flows through diodes D_A and D_B with the slope V_{o2}/L. In short, when the switch Q_1 is in ON state, energy is stored in the inductor; when Q_1 is in OFF state, power is delivered to one of the outputs, depending on the state of switch Q_2.
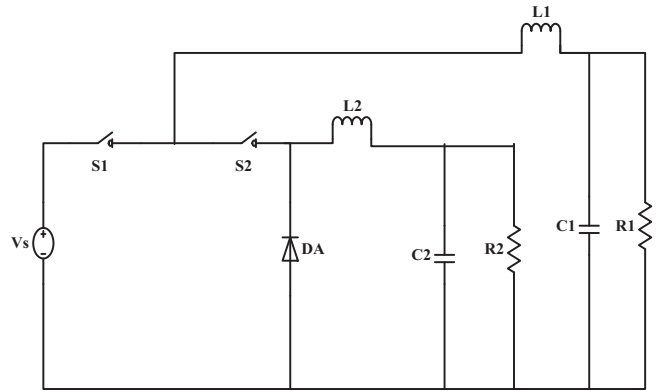
Three different methods of converting single out put converter to dual output converter are discussed and compared [34]. A simple method is to use time multiplexing of inductor current. In this method different switches conduct inductor current to their output voltages for a fraction of time. In the other method, output energy is drawn from the complementary terminals of the inductor. The third method is to use switched nodes to charge capacitors. A family of single input multioutput DC–DC converters synthesized from boost converter for step up and step down applications is presented in [36]. A concept of single energizing cycle and multiple energizing cycles per switching period for smooth flow of energy is discussed in [37]. Design and control of a dual output buck converter is explained in [38]. In this approach, the number of switches is reduced thus reducing the overall cost of the converter. The problems like large ripple and cross regulation of output voltages associated with single inductor dual output buck converter have been addressed and methods to supress these problems have been discussed in [39]. A single

Fig. 12. Single input–double output unidirectional buck converter.

inductor multioutput buck converter with two outputs V_{01} and V_{02} is shown in Fig. 11. These output voltages are regulated by adjustment of duty cycles d_1 and d_2. Steady state output input relation is given by:

$$\frac{V_{o,1}}{V_{in}} = \frac{d_1 d_2 R_1}{d_2^2 R_1 + (1 - d_2)^2 R_2} \tag{5}$$

$$\frac{V_{o,2}}{V_{in}} = \frac{d_1 (1 - d_2) R_2}{d_2^2 R_1 + (1 - d_2)^2 R_2} \tag{6}$$

and duty cycles are determined by

$$d_1 = \frac{I_{o,1}}{I_{o,1} + I_{o,2}}, \quad I_{o,1} + I_{o,2} = I_L \tag{7}$$

$$d_2 = \frac{V_{o,1}[d_2^2 R_1 + (1 - d_2)^2 R_2]}{V_{in} d_2 R_1} \tag{8}$$

The main focus of this approach to reduce cross regulation problem by using a multivariable digital controller [40]. Satisfactory performance of this controller is verified by simulation and experimental results. Design methodologies of a multi-output converter are presented and verified for four output converter with 86% efficiency. These methodologies are claimed to be

suitable for unlimited number of outputs [41]. A model, design and control of a dual output buck converter with reduced devices and unidirectional/bidirectional characteristics for motor drive system applications is presented [42,43] as shown in Figs. 12 and 13. Simulation and experimental results are provided to prove better power loss distribution and high efficiency with low count

switching devices. The drawback of this converter is that it requires high current rating switches as compared to the converters in [36,37].

2.3. Multiinput–multioutput converters

A multi-input–multi-output buck–boost DC–DC converter derived from buck–boost converters in matrix format is suggested in [44]. This converter is used to interface DC loads and various DC input sources in a microgrid on controlled power sharing concept. The input sources are used in various range of power and voltage and output voltages varies from the values lower than the minimum input or greater than the maximum value. Analysis with simulation results has been presented. Fig. 14 shows the circuit diagram of the proposed system. The number of inputs and outputs are claimed to be unlimited. However the input sources are unable to power up outputs simultaneously.

Three port converters have attracted interest in the recent research. A typical three port converter consists of a voltage source port, a storage unit port and an output or load port. This converter can operate in three modes i.e. dual input, dual output and single input–single output mode. It acts as a dual input converter if both battery and input source are delivering the power to the load.
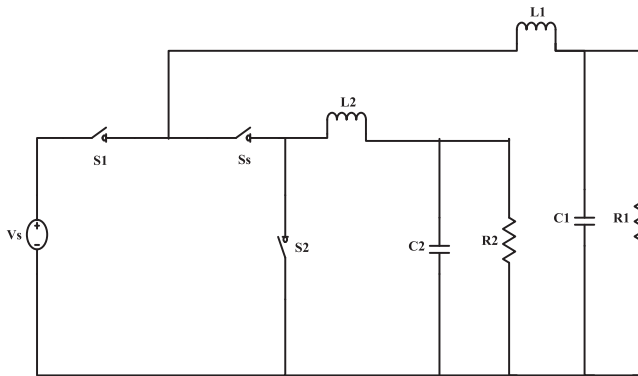

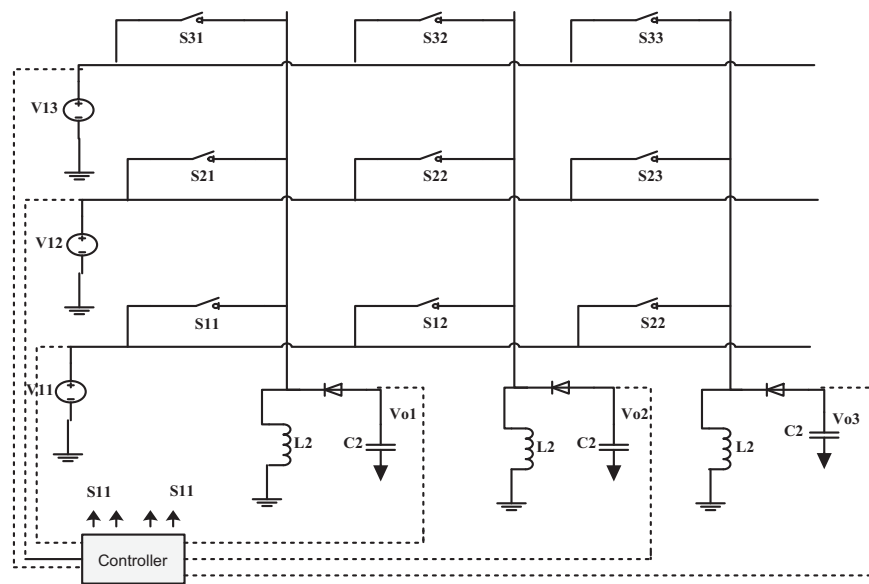**Fig. 13.** Single input–double output bidirectional buck converter.

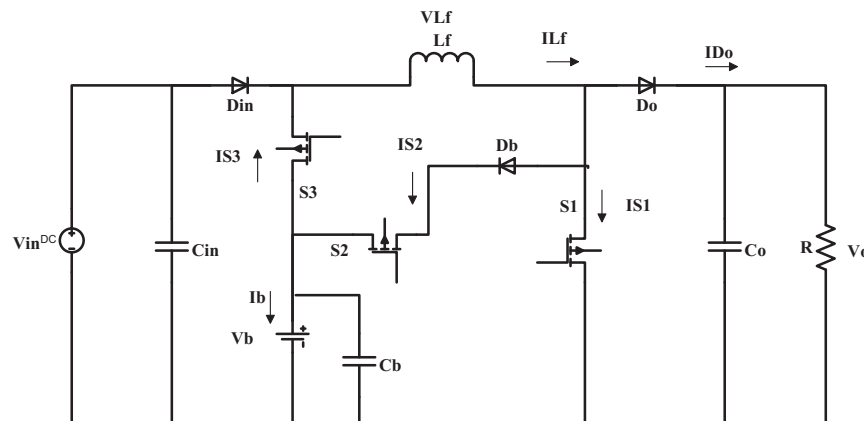**Fig. 14.** Multiinput–multioutput converter topology.

Fig. 15. Three port converter.

If the power is consumed by the load and battery, the converter is in its dual output state. Input source or battery can power up the load in single input–single output mode. This topology has advantages like high efficiency, compact size, reliability and good power management. Due to these advantages these are widely used in renewable energy systems. A non-isolated three-port converter to interface PV, battery and load is presented in [45]. With less conversion stages, higher power density and reliability are achieved and are verified by experimental results. A family of non-isolated three port converters is introduced in [46,47]. These three port converters are generated by introducing a single input–single output converter in a dual input or dual output converters. Method to systematically derive multi-port converter with DC link inductor concept is presented in [48] and a family of multi-port converter topology is presented. Another systematic approach for derivation of three port converters from dual input and dual output converters is explained in [49]. Several three port converter topologies (TPC) have been generated by this procedure and a boost type TPC as shown in Fig. 15 is analyzed in dual input, dual output and single input–single output mode.

2.3.1. Dual output mode

A three port converter in dual output mode is shown in Fig. 16. In this mode, switch S_3 is kept OFF. Three switching states are explained in one switching period. Current and voltage waveforms are shown in Fig. 17.

Switching State I: switch S_1 is ON and S_2 is OFF. Inductor L_f absorbs energy from input voltage V_{in} and its current I_{Lf} increases.

$$\frac{dI_{L_f}}{dt} = \frac{V_{in}}{L_f} \tag{9}$$

Switching State II: switch S_1 is OFF and S_2 is ON. Battery is charged by both V_{in} and inductor L_f and its current I_{Lf} decreases.

$$\frac{dI_{L_f}}{dt} = \frac{V_{in} - V_b}{L_f} \tag{10}$$

Switching State III: both the Switches are OFF. Load is powered by V_{in} and release of energy by inductor L_f and its current I_{Lf} decreases.

$$\frac{dI_{L_f}}{dt} = \frac{V_{in} - V_o}{L_f} \tag{11}$$

By applying inductor volt–second balance theorem on inductor in steady state continuous-conduction mode we get the input output voltage relationship as

$$(V_{L_f})_{Ts} = V_{in} - V_b D_2 - V_o(1 - D_1 - D_2) = 0 \tag{12}$$

$$V_{in} = V_o(1 - D_1) - V_b D_2 \tag{13}$$

or

$$V_o = \frac{V_{in} - V_b D_2}{1 - D_1 - D_2} \tag{14}$$

or

$$V_b = \frac{V_{in} - V_o(1 - D_1 - D_2)}{D_2} \tag{15}$$

where D_1 and D_2 are the duty cycles of the switches S_1 and S_2, respectively, V_b is the battery voltage and V_o is output voltage.
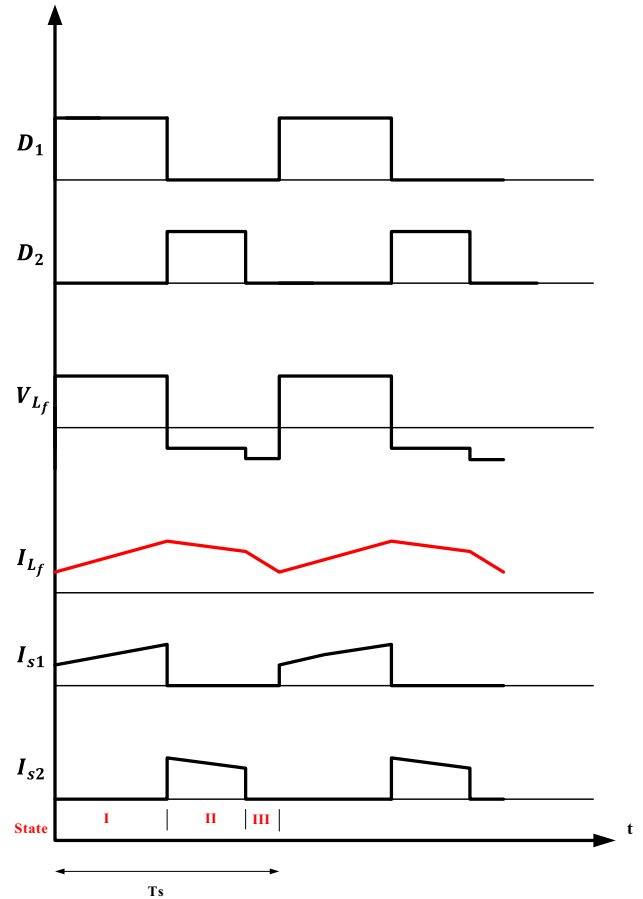

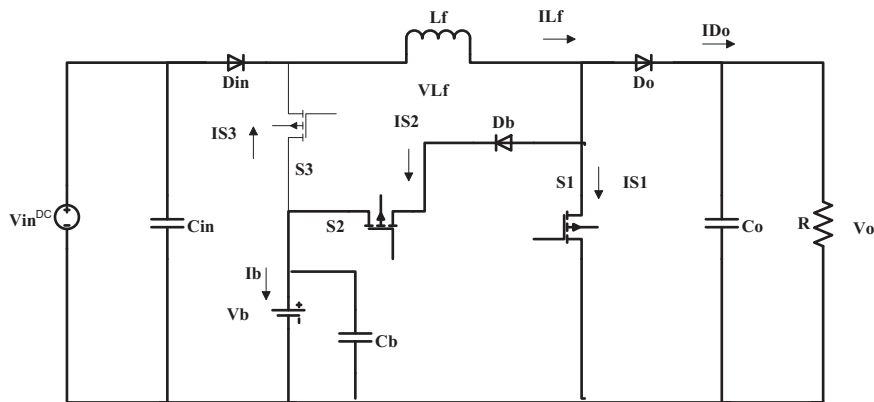**Fig. 17.** Typical waveforms of three port converter in dual output mode.

Fig. 16. Equivalent circuit of three port converter in dual output mode.
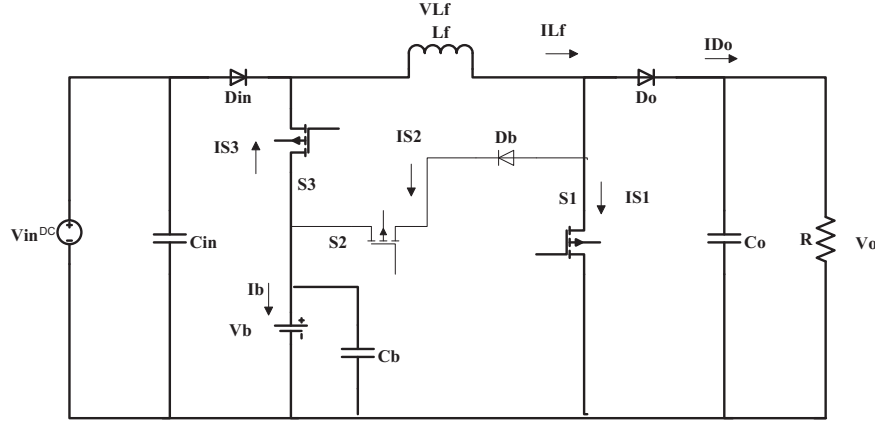
Fig. 18. Equivalent circuit of a three port converter in dual input mode.
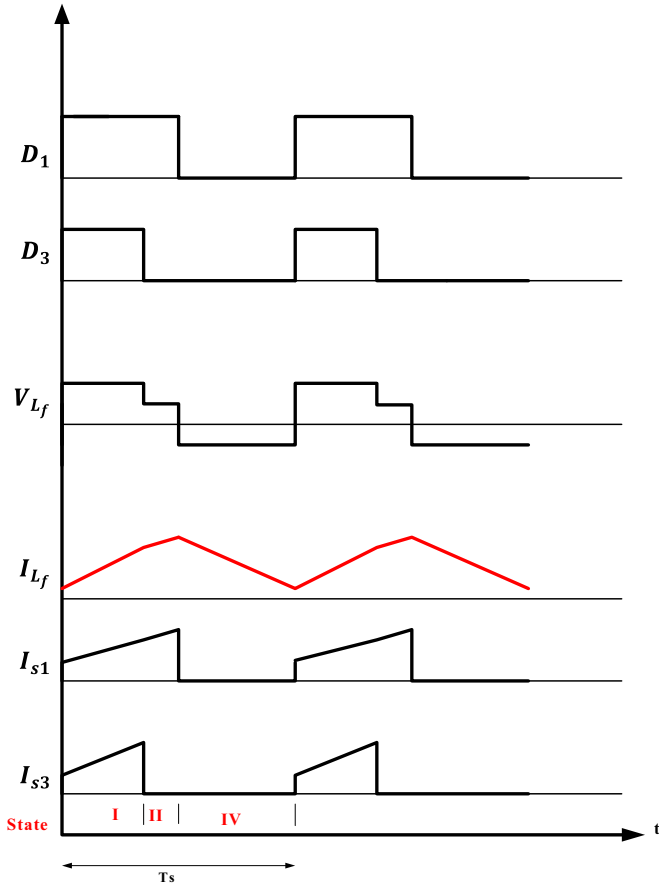

Fig. 19. Typical waveforms of a three port converter in dual input mode.

2.3.2. Dual input mode

A three port converter in dual output mode is shown in Fig. 18. Four switching states are explained in one switching period. Voltage and current waveforms are shown in Fig. 19.

Switching State I: switch S_1 and S_3 are ON. Inductor L_f absorbs energy from battery voltage V_b and its current I_{L_f} increases.

$$\frac{dI_{L_f}}{dt} = \frac{V_b}{L_f} \tag{16}$$

Switching State II: switch S_1 is ON and S_3 is OFF. Inductor L_f absorbs energy from input voltage V_{in} and its current I_{Lf}

increases.

$$\frac{dI_{L_f}}{dt} = \frac{V_{in}}{L_f} \tag{17}$$

Switching State III: switch S_1 is OFF and S_3 is ON. Load is powered by V_b and release of energy by inductor L_f and its current I_f decreases.

$$\frac{dI_{L_f}}{dt} = \frac{V_b - V_o}{L_f} \tag{18}$$

Switching State IV: both the switches are OFF. Load is powered by V_{in} and release of energy by the inductor L_f and its current I_{Lf} decreases.

$$\frac{dI_{L_f}}{dt} = \frac{V_{in} - V_o}{L_f} \tag{19}$$

By applying inductor volt–second balance theorem on inductor in steady state continuous-conduction mode we get the input–output voltage relationship as

$$V_{in} = \frac{V_o(1 - D_1) - V_b D_3}{1 - D_3} \tag{20}$$

$$V_o = \frac{V_{in}(1 - D_3) - V_b D_3}{1 - D_1} \tag{21}$$

2.3.3. Single input–single output mode

The equivalent circuit in the single input–single output mode is shown in Fig. 20. In this mode switch S_2 is kept OFF and S_3 is kept ON. The battery supplies the load alone and converter acts as a conventional boost converter.

A multiinput DC–DC boost converter combining the multiple sources in a unified structure with five switching periods is introduced in [50]. This system is also capable of providing reactive power to the load and grid. Different features have been verified by simulation results. A three-input DC–DC boost converter (Fig. 21) is presented in [51]. It has one bidirectional port in addition to two one directional input ports. This topology has been reported useful for integration of hybrid energy system having storage element and supplying the load individually or simultaneously. Four power switches are used with independent control and different duty cycles to provide regulated output. The validity of this converter and control system has been verified by simulation and experimental results for different conditions of operation. Simulation results show good transient and steady state responses of the converter with respect to step changes in generation and the load requirement. The simulation results have been verified
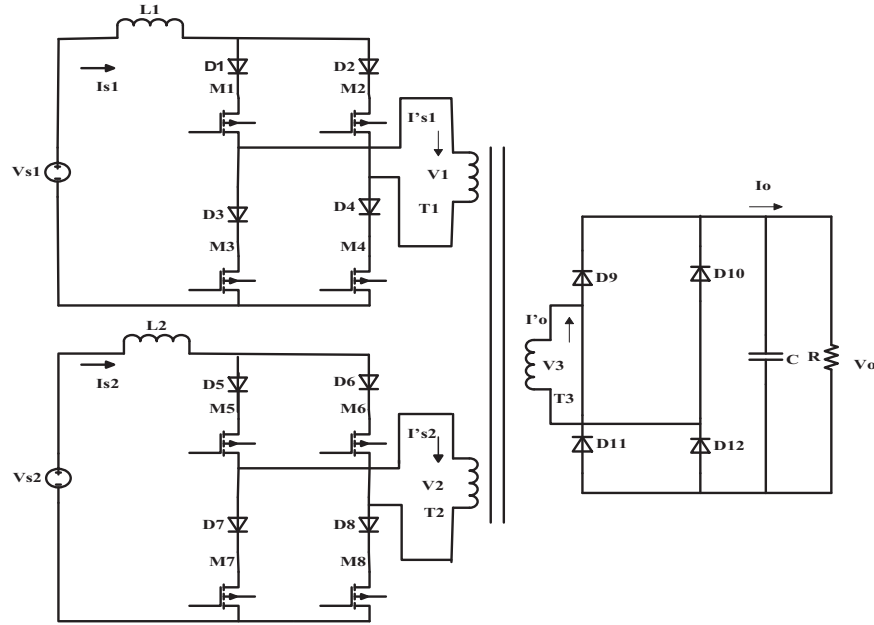
Fig. 20. Three port converter in single input–single output mode.

Fig. 21. Three input DC–DC converter.

Table 1
Comparison of multiinput DC–DC converter topologies.

Topology	Cost	Reliability	Flexibility	Efficiency
MI buck	**	**	**	***
MI boost	***	**	***	****
MI buck–boost	*	*	**	*
MI Cuk	*	*	****	*
MI SEPIC	*	*	****	**

by a low power prototype with an acceptable efficiency. A single inductor multiinput–multioutput DC–DC boost converter for hybrid electric vehicles is proposed by Nahavandi et al. [52]. The converter has multiinput–multioutput interface however both the input sources cannot power up the load simultaneously. A single inductor dual input–dual output converter considering battery as a second source is presented in [53]. However battery charging circuit is not controlled in this topology.

3. Comaprison of multiinput non-isolated DC–DC converter topologies

Each non-isolated DC–DC converter topology has its own merits and demerits therefore there are no specified selection criteria to choose any specific topology for any particular application. However these topologies can be compared under certain characteristics like cost, reliability, flexibility and

efficiency. The comparison is made only on the bases of simple synthesized topology. Control schemes and extra cells added to achieve additional benefits are not taken into account in this comparison.

3.1. Cost of converter

The expected cost of the converter can be worked out by the number of components being used in the particular topology. Multiinput converters share the components in their input and output stages therefore they have advantage of less cost as compared to the independent single input converters. Similarly non-isolated converters do not require bulky transformers for input–output isolation therefore their cost is less as compared to isolated converters. Among non-isolated topologies, buck and boost converters are less costly as compared to the others due to less number of components in their circuitry. Among these two topologies, boost converters have an edge over the buck. Xiao et al. [54] found that the boost converter has the following advantages over the buck in photovoltaic applications:

- Current rating of MOSFET in boost converter is lower as compared to buck converters.
- Boost converters require high inductance to achieve current ripple as compared to buck converters.
- Buck converters require a large capacitor to smooth discontinuous input current.
- Freewheeling diode can serve as a blocking diode in the boost converter, however this is an additional component in buck.

Fig. 22. Two input current fed full bridge converter.

3.2. Reliability

Reliability of the converters can be determined by two factors. One factor is the number of common components in the circuit and other is the stress on each component. Buck–boost, Cuk and SEPIC converters have more number of passive devices and have high electrical stress on components like switches, diodes and capacitors, therefore these topologies are less reliable as compared to buck and boost converters [55,56].

3.3. Flexibility

Flexibility can be defined as the compatibility of the topology with different kinds of input sources. As the main objective of multiinput converters are to combine different input sources to provide the desired output therefore the topology input interface is very important. The topology should be able to integrate different input sources and provide wide range of output voltages. Cuk and SEPIC converters are better in flexibility as their input currents are continuous and ripple free and at the same time these are able to step up or step down the input voltage [57,58].

3.4. Efficiency

In terms of efficiency buck and boost converters are considered as the most efficient topologies among the non-isolated category [57,59].

Table 1 shows a comparison of non-isolated DC–DC converter topologies. The table is explained as, the "∗" sign shows the attribute of topology under the each heading. More numbers of "∗" signs indicate that the topology is better as compared to others i.e. "∗∗∗" is better than "∗∗" which is better than "∗".

Fig. 23. Typical current and voltage waveforms for two input full bridge converter.

4. Multiinput isolated DC–DC converters

Topologies of non-isolated converters are Fly Back, Forward, Push Pull, Full Bridge and Half bridge converters [60]. Forward and Fly Back converters are used for low voltage and low power applications. 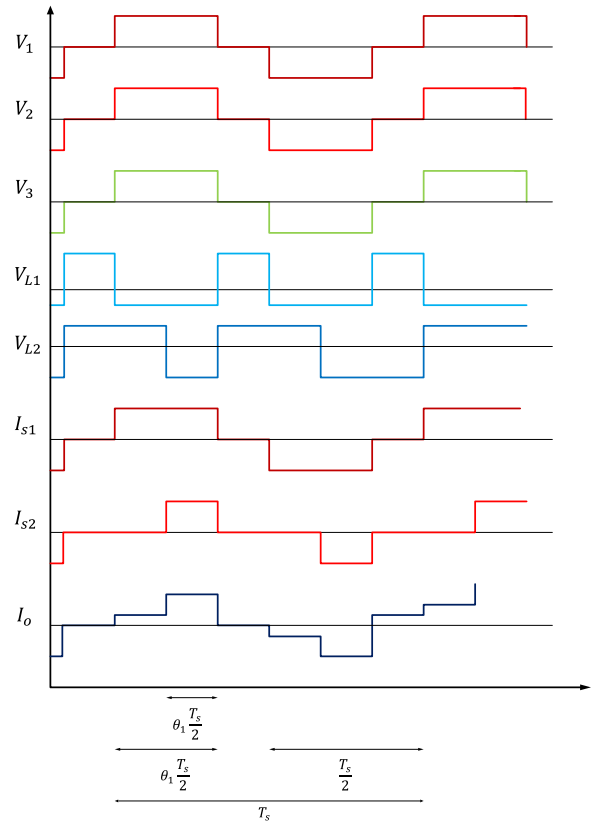But in high power density and high output voltage applications, these are not suitable. As discussed in the section above, the non-isolated converters are preferred over isolated converters in low voltage/low power applications therefore Fly back and Forward converters will not be discussed in the present work. In medium to high voltage and power applications, bridge converters (half bridge, full bridge) are more suitable [61]. Therefore these have been examined in detail.

4.1. Multiinput full bridge converter

A family of a multiport bi directional DC–DC converters is presented in [62] a general method to integrate multiple sources is defined. Multiple sources are interconnected without addition of extra conversion stages or switches and are controlled by digital controller. A multiport structure for hybrid power sources utilizing single power processing stage presented in [63]. Using bidirectional switches and magnetic coupling several multiport bidirectional topologies proposed are extended to poly-phase interleaved versions to integrate source, load and storage. A method for synthesis of multiinput isolated DC–DC converter is explained with the introduction of pulsating voltage cells [28]. A multi-input full bridge DC–DC converter with a multiwinding transformer and based on addition of flux is shown in Fig. 22. This converter combines two input sources of different amplitudes by adding the magnetic flux produced in transformer core. It consists of two current sources, a three winding transformer and an output port. The number of input sources can be increased while the output port and the coupling transformer remain the same. Magnetic flux is produced by input current sources through current fed DC/AC inverter. Each switch of AC/DC inverter has a diode in series which blocks the reverse current to ensure the simultaneous transfer of power from both the sources. Input and output stage windings are wound on the same core so that the flux linked by each source can entirely pass through the output stage winding. The output stage consists of an AC/DC rectifier and filters. Transfer of power takes place when the switches at the diagonal position of full bridge converter are turned ON. The power is not transferred when two consecutive switches of either leg of full bridge converter are turned ON. This is called free-wheeling state of the converter. A phase shift PWM scheme in implied to control. Twelve modes of operation are explained [12,64,65]. Voltage and current waveforms are shown in Fig. 23. Steady state average voltage across the inductor is given by:

$$V_{L1} = \left(V_{s1} - \frac{n_1}{n_3}V_o\right)\theta_1\frac{T_s}{2} + V_{s1}(1-\theta_1)\frac{T_s}{2} = 0 \qquad (22)$$

where n_1 and n_3 are the number of turns for first and third windings of the transformer, V_{s1} is the input voltage of source one, V_{L1} is the voltage across the inductor, θ_1 is the phase shift percentage for input source one, V_o is the output voltage and T_s is the time of switching.

The relationship between input source one and output voltage can be derived as

$$V_{s1} = \frac{n_1}{n_3}\theta_1 V_o \qquad (23)$$

Similarly the relationship between input source two and output voltage can be derived as

$$V_{s2} = \frac{n_2}{n_3}\theta_2 V_o \qquad (24)$$

where θ_2 is the phase shift percentage for second input source.

This converter can deliver power individually and simultaneously however the reverse current blocking diode connected in series with the switch eliminates the chance of converter's operation in bidirectional mode. Furthermore large number of switches and complex controller increases the cost, reliability and size of the converter. A converter with less components, simple in configuration, low cost and high efficiency for high voltage output applications is presented in [66]. Another simplified multiinput full bridge DC–DC converter is proposed and analyzed by Yang et al. [67]. In this configuration the power switches are switched out of phase with a double phase-shift control strategy and the switches with simultaneous turn OFF are shared. This control scheme reduces switching devices which makes the circuit simple. Voltage-fed controlled dc sources can deliver energy to load individually and simultaneously with soft-switching technology. Converter structure is shown in Fig. 24 and key waveforms are shown in Fig. 25. A high step-up, high voltage bidirectional dual input current source type isolated converter is investigated by Wai et al. [68]. To avoid the switching voltage spikes introduced by leakage inductance, an active clamping circuit is used and to reduce output voltage ripple this configuration applies a pulse width modulation interleaved method. Three states of operation are examined to achieve the advantages like soft switching, isolation between source and load, bidirectional operation, high efficiency and high voltage step up ratio.

A ZVS full-bridge DC–DC converter with two additional switches to interrupt circulating current is able to achieve high efficiency and excellent power regulation as reported in [69]. A method for reducing the components of soft switching multiinput converters is addressed by Yu and Kwasinki [70]. An input cell reduction method is introduced first by inserting a reverse blocking capacitor between input legs which eliminates the condition of symmetric duty cycles to maintain the balance voltage at magnetizing
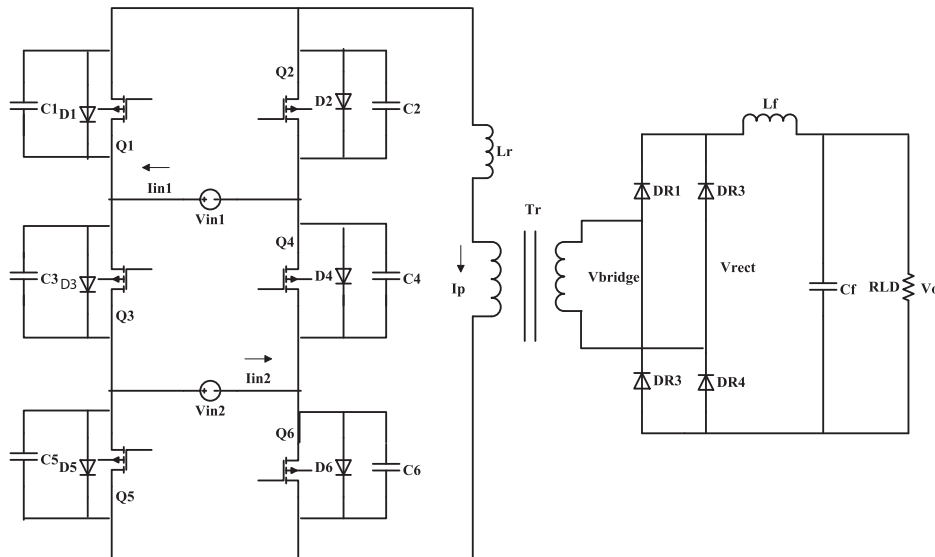

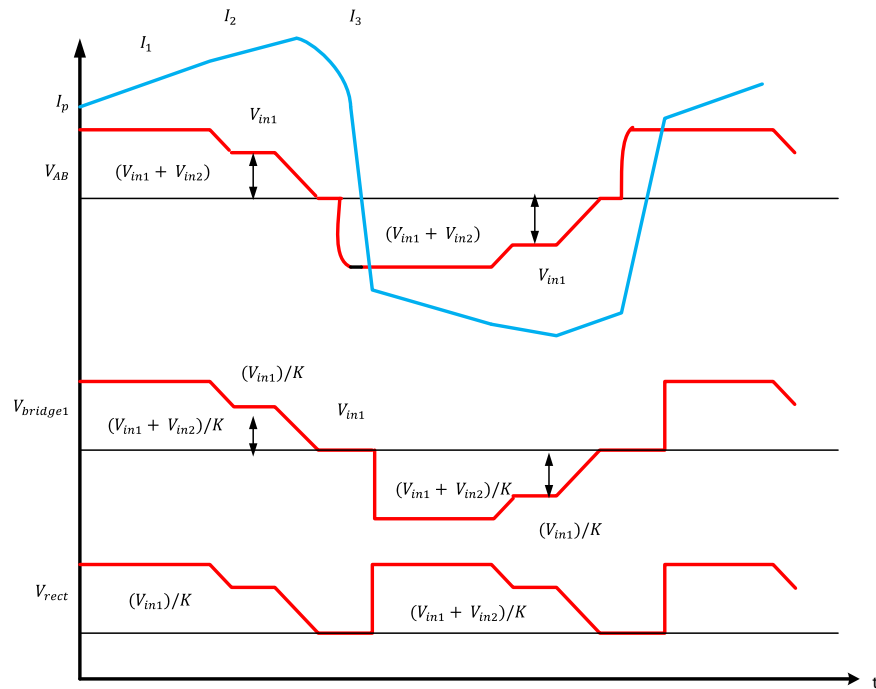**Fig. 24.** Double input full-bridge DC–DC converter simplified form.

Fig. 25. Key waveforms of full bridge converter with two sources.
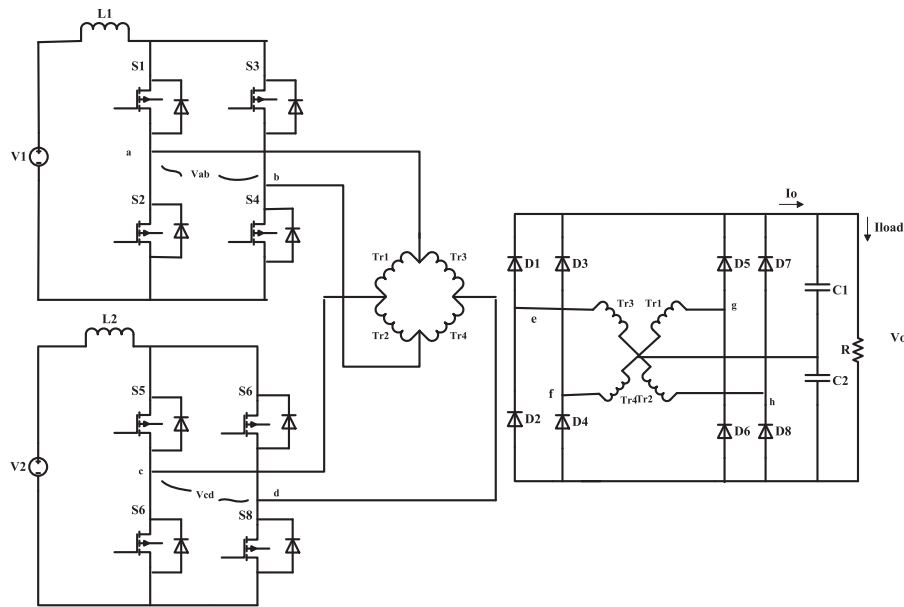

Fig. 26. Dual input current fed DC–DC converter.

inductor. Two new topologies of multiinput converters are derived with fewer components as compared to the conventional ones. A two input current fed DC–DC converter based on four transformers interconnection structure is proposed for fuel cell and super capacitor applications [71,72] as shown in Fig. 26. Interleaved pulse width modulation scheme along with new method for transformer interconnection are used to deliver energy to high voltage DC bus. Analyses have been carried out in dual and single output mode. In order to improve the performance of the proposed converter, methods to increase the number of inputs and reduce the magnetic elements are also discussed. The converter has two independently controlled input ports with low input current ripple. The transformers are shared by both the inputs but winding connections of four transformers are complex to handle.

A systematic approach to convert a single port full bridge converter to three port is explained in [73] A multiport isolated DC–DC converter for hybrid storage system is presented in [74], the converter is able to achieve zero voltage switching for all switches with bidirectional power flow and low current ripples, however the operation modes of the converter are not fully explained.

4.2. Multiinput half bridge DC–DC converters

The half-bridge converter (HBC) is one of the basic topologies with isolation and the primary switches are usually operated alternately or complementary while the input capacitors in a HBC can be regarded as voltage sources. When the two switches
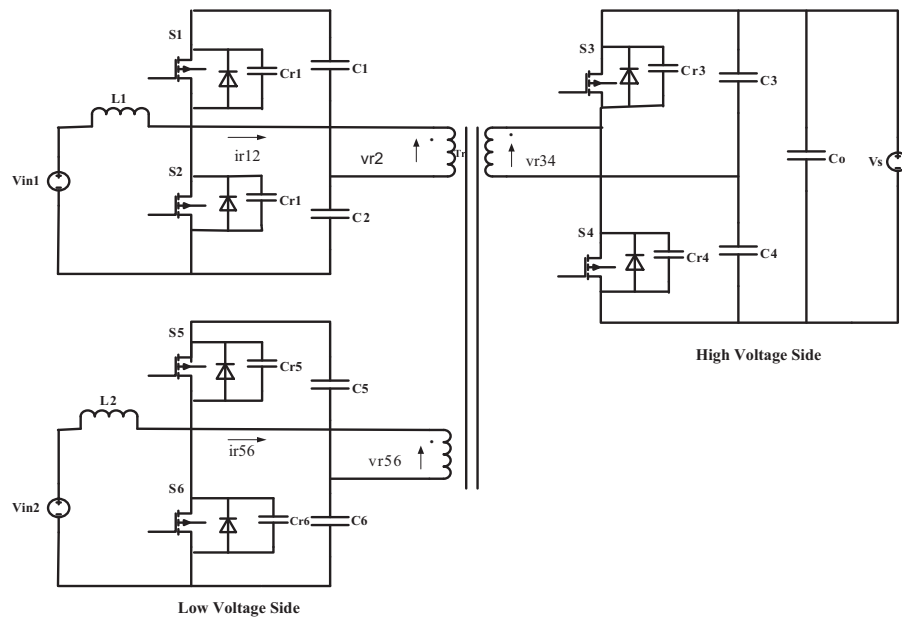
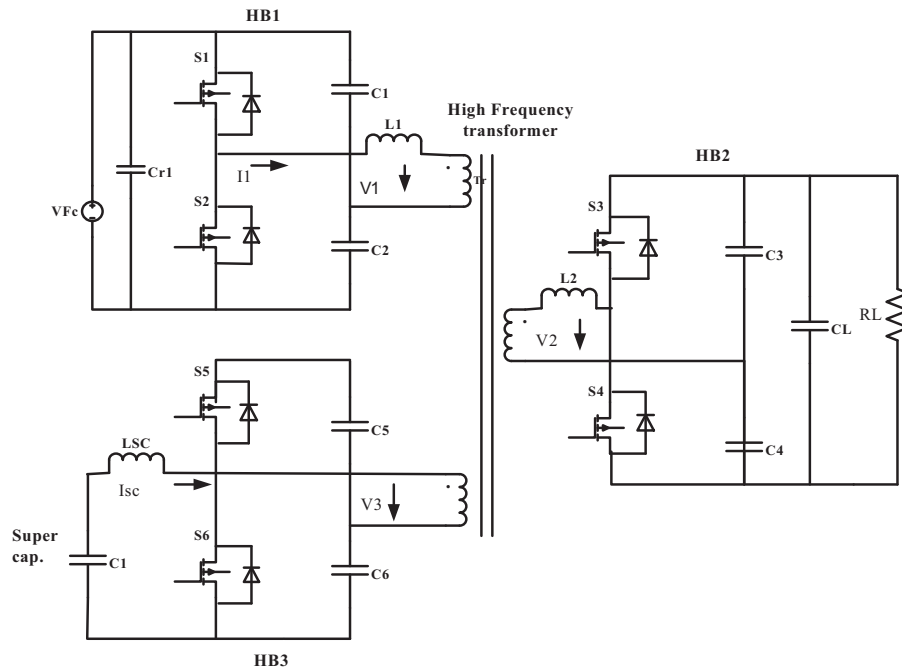**Fig. 27.** Multiinput ZVS bi-directional DC–DC converter.

Fig. 28. Triple half-bridge bidirectional DC–DC converter.

are driven with symmetrical signals, which are identical to each other with 180-degree phase shift, the converter is called symmetrical half bridge. For the one with complementary driving signals, it is called asymmetrical half bridge.

A bi-directional DC–DC converter comprising of three half bridges is presented in [75] and shown in Fig. 27. The converter is used to interface multiple energy storage elements with two half bridges on low voltage side and one half bridge on high voltage side. This converter can deliver the power in either directions with different voltage levels and can achieve soft switching and has less number of components and high efficiency as compared to the multiinput full bridge topologies. Control analysis and dynamic design of this converter is presented with double loop control system in [76]. However in case of mismatch between source and load voltage and under light load conditions,

zero switching cannot be achieved due to wide variation of voltages [77].

A multiinput bi-directional converter using boost half bridge cells is used to handle voltage variations at the ports using phase shift and duty cycle control and it also minimizes switching and conduction losses in a fuel cell based generation system [78] and in a photovoltaic plus battery storage system in [79]. This concept is further elaborated in a three port converter as shown in Fig. 28 using one boost half bridge and two other half bridges. These bridges generate high-frequency voltage controlled by a phase angle and this high frequency voltage is applied to corresponding winding of the high frequency transformer. The advantage of phase shift plus pulse width modulation control is over phase shift control, as proposed in [57], is that peak and rms values of current are reduced however as all the ports are controlled by
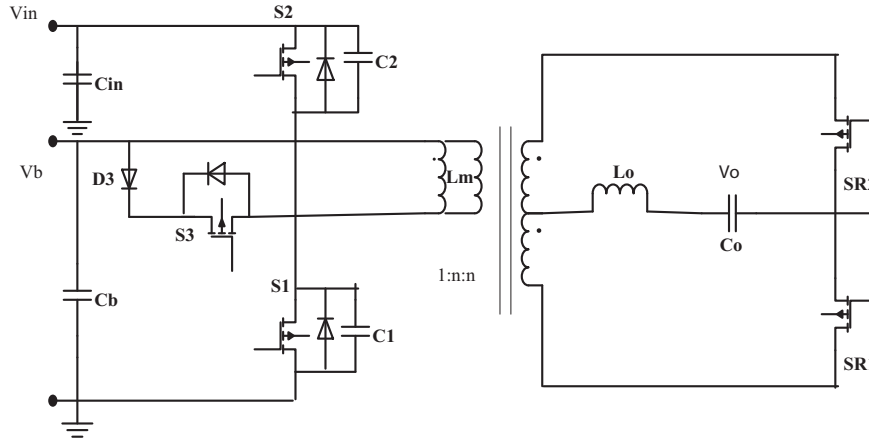
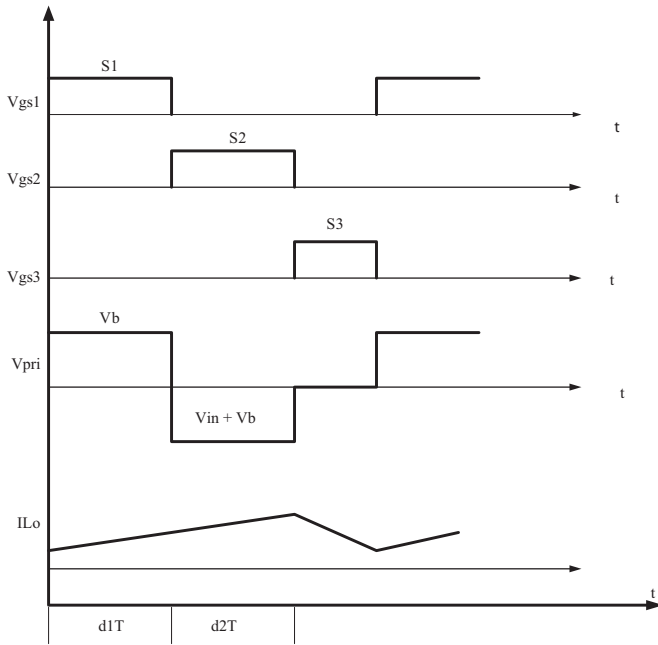**Fig. 29.** Three Port modified half bridge topology.

Fig. 30. Steady state waveforms for three port half bridge topology.

same duty cycle, only one port voltage is allowed to vary in this control scheme as compared to volt–second balance control method where all the port voltages may vary. As the high frequency current passes through the half bridge capacitors therefore this converter is not suitable for high power applications [80]. Xie et al. [81] examined a half bridge multiinput converter is with dual close loop and decoupling network control scheme to obtain better dynamic response.

A tri-modal three port half bridge converter is obtained by adding one middle branch to a two port half bridge converter to achieve zero voltage switching and bi-directional properties [82,83]. Converter structure is shown in Fig. 29 and waveforms are shown in Fig. 30. The work is further extended to design a system level control strategy in a satellite platform power system in [84]. Modeling and control of three port converter using decoupling network presented in [82–84] is further elaborated for satellite applications in [10]. The steady state relationship between voltages of different ports in continuous conduction mode can be obtained by applying volt–second balance theorem on primary and secondary side inductors.

On primary side:

$$V_{bi}D_1 = (V_{in} - V_{bi})D_2 \qquad (25)$$

which gives battery voltage

$$V_{bi} = \frac{D_2}{D_1 + D_2}V_{in} \qquad (26)$$

where V_{bi} is battery voltage, V_{in} is the input voltage D_1 and D_2 are the duty cycles of switches S and S_2

Similarly applying volt–second balance on secondary side inductor gives:

$$D_1T(nV_{bi} - V_o) + D_2T(nV_{in} - nV_{bi} - V_o) - (1 - D_1 - D_2)TV_o = 0 \qquad (27)$$

$$V_o = 2\frac{D_1D_2}{D_1 + D_2}nV_{in} \qquad (28)$$

where V_o is output voltage, n is the turn ratio for the transformer and T is the switching time.

The steady state currents can be obtained by applying power conversion principle by assuming lossless converter:

$$V_{in}I_{in} = V_{bi}\,I_{bi} + V_oI_o \qquad (29)$$

where I_{in} is average input current I_{bi} is the battery current and I_o is the load current.

A three-port half-bridge converter derived from integration of half-bridge and forward fly back converters and synchronous rectifiers is presented in [85], shown in Fig. 31 and key waveforms are shown in Fig. 32. The primary circuit of half bridge and fly back converters act as a buck converter to interface renewable energy source and a storage device. The advantages of this integrated converter are lower number of components, low cost, small size and weight as no extra components are added in basic half bridge structure. The control system is comprised of pulse width modulation (PWM) and feedback control structure. Converter is suitable for hybrid energy system where extra available energy is stored in the battery. It can operate in three modes i.e. dual input, dual output and single input mode. In dual output mode there are three switching states are explained in one switching period.

Switching State I: before this state switches S_3 and S_4 are ON and S_1 and S_2 are OFF. The inductor current freewheels through S_3 and S_4. In this state S_1 is switched ON and S_4 is turned OFF. A positive voltage is applied across the transformer and current through the magnetizing inductor of the transformer is given by:

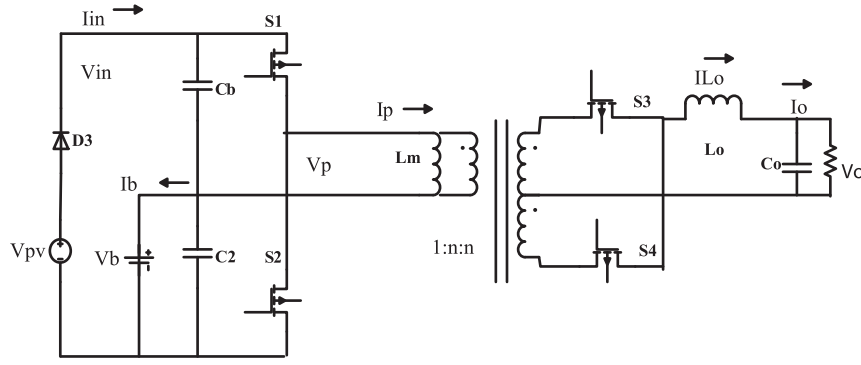$$\frac{dI_{L_m}}{dt} = \frac{V_{in} - V_b}{L_m} \qquad (30)$$

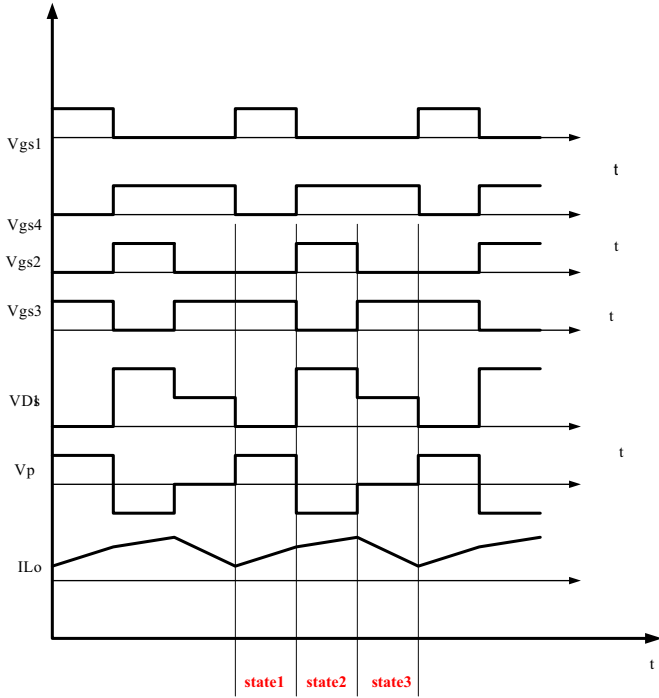**Fig. 31.** Three port half bridge converter.

Fig. 32. Waveforms of three port half bridge topology.

and the current through the output inductor is

$$\frac{dI_{L_o}}{dt} = \frac{n(V_{in} - V_b) - V_o}{L_o} \tag{31}$$

and the total current on primary side is

$$I_p = I_{Lm} + nI_{lo} \tag{32}$$

Switching State II: switches S_1 and S_3 are turned OFF and S_2 and S_4 are switched ON. A negative voltage applies at the primary winding of the transformer and the inductor currents are

$$\frac{dI_{L_m}}{dt} = \frac{-V_b}{L_m} \tag{33}$$

$$\frac{dI_{L_o}}{dt} = \frac{n(V_{in} - V_b) - V_o}{L_o} \tag{34}$$

and the total current on primary side is

$$I_p = I_{Lm} - nI_{lo} \tag{35}$$

Switching State III: the switch S_2 is OFF and S_3 is ON. In this state primary voltage is clamped to zero and the currents I_{L_m} and I_{L_o} are freewheeled by switches S_3 and S_4.

$$\frac{dI_{L_m}}{dt} = 0 \tag{36}$$

$$\frac{dI_{L_o}}{dt} = \frac{-V_o}{L_o} \tag{37}$$

$$I_p = 0 \tag{38}$$

By applying inductor volt–second balance theorem on magnetizing inductor of the transformer and output filter inductor in steady state continuous-conduction mode we get the input–output voltage relationship as

$$V_{in} = \frac{(D_1 + D_2)V_b}{D_1} \tag{39}$$

$$V_o = n[D_1(V_{in} - V_b) + V_b D_2] = 2nD_{2V_b} \tag{40}$$

where D_1 and D_2 are the duty cycles of the switches S_1 and S_2, V_b is battery voltage and V_o is output voltage.

A multiinput converter developed from boost half bridge and full bridge cells is presented with the features like dual input ability, reduces number of power devices, high voltage conversion ratio as compared to boost converter and ZVS operation [86]. The disadvantages of this converter are its complex design and control system. A series asymmetrical half-bridge converter is presented for high-voltage and power applications [87]. It consists of two series half-bridges with a shared primary leakage inductance, transformer, and secondary rectifier. The advantages of this topology are that the voltage stress across the switch is reduces to half of the input voltage, switching losses are reduces by ZVS for all switches and voltages across input capacitors are balanced automatically. This topology can be extended for multiinput applications. A current fed multiresonant bi-directional half bridge DC–DC converter is presented in [88]. The major advantages of this converter are low input current ripple, high step up capability and low active switches however the phase shift controlling of the converter is not explained.

5. Challenges and future scope of work

Multi-input converters have made tremendous improvement in the past few years. However literature review suggests that there are some limitations still to be addressed. These limitations are elaborated below and also summarized in Table 2.

- Multiinput converters and can deliver the power individually and simultaneously to the load, however during the light load

Table 2
Limitations in multi-input DC–DC converters.

Converter topology	Cited references	Limitations
Multi-input	[14–18,20–32,66–71,76,81,86]	No energy storage device
	[15,19,44,52]	No simultaneous energy transfer
	[18,19]	High power loss, low efficiency, high number of components
	[50,51]	Complex control, bigger size, high cost
Multi-output	[33–43]	Only one input source, no storage device
Three port	[45–49,73,78–80,82–84]	Less reliable (only one source)

conditions and/or when both the sources are available, no storage device is present to store the extra available energy [14–18,20–32,66–71,76,81,86].

- Only one source can power up the load at a time [15,19,44,52].
- High power loss, low efficiency, and more number of switches [18,19].
- Low efficiency [29–31].
- Only one renewable energy source (less reliable) [45–49,73,78–80,82–84].
- Increased size and cost due to two inductors [50,51].
- Unidirectional operation, no storage port [15,64,65].
- Too many active switches and complex control system [70,71].

Renewable energy sources are expected to be the major shareholder in future power generation industry. Efficient and reliable power electronics interface is required. Several power electronics converters have been presented in the above study to independently address the issues like high multiinput–multioutput interface, high efficiency, reliability, low cost, minimum number of components and less power loss, but no single circuitry is available which can collectively address these issues. Further research is required to develop a circuitry which can provide a good match between instantaneously changing sources and variable loads.

6. Conclusion

Several multiinput DC–DC converters topologies have been presented in the literature. General rules for converting single input converters to multiinput converters have been reviewed. Synthesis of multiinput converters has been discussed. Literature suggests that multiinput converters have reduced the problems associated with single input converters and enhanced the interface of different renewable sources which can deliver power individually and simultaneously to the load. The use of multiinput converters in renewable energy applications and hybrid vehicles has reduced the cost for integration due to their minimum components and reduced switching losses with the use of lossless soft switching circuits and has increased reliability and power security. Three port converters have gained popularity in renewable energy applications. This concept of three port converters can be further enhanced to the development of multiinput–multioutput converters for renewable energy and hybrid vehicle applications. However the study of different multiinput DC–DC converter topologies suggests that there is no single topology which can handle the entire goals of cost, reliability, flexibility and modularity single handed. Efforts are continued to make multiinput converters and their control schemes more efficient and cost effective for integration of renewable energy sources and other applications.

References

[1] Hui J, Bakhshai A, Jain PK. A hybrid wind–solar energy system. A new rectifier stage topology. In: Proceedings of the IEEE applied power electronics conference and exposition; 2010. pp. 155–161.

[2] Kim S, Jeon J, Cho C, Ahn J, Kwon S. Dynamic modeling and control of a grid-connected hybrid generation system with versatile power transfer. IEEE Trans Ind Electron 2008;55(4):1677–88.

[3] Chauhan A, Saini RP. A review on integrated renewable energy system based power generation for stand-alone applications: configurations, storage options, sizing methodologies and control. J Renew Sustain Energy Rev 2014;38:99–120.

[4] Reddy KS, Kumar M, Mallick TK, Sharon H, Lokeswaran S. A review of integration, control, communication and metering (ICCM) of renewable energy based smart grid. J Renew Sustain Energy Rev 2014;38:180–92.

[5] Jiang W, Fahimi B. Multi-port power electric interface for renewable energy sources. In: Proceedings of the IEEE applied power electronics conference; 2009. pp. 347–352.

[6] Chen Y, Huang AQ, Yu X. A high step-up three-port dc–dc converter for stand-alone PV/battery power systems. IEEE Trans Power Electron 2013;28(11):5049–62.

[7] Zhang Z, Pittini R, Andersen MAE, Thomsena OC. A review and design of power electronics converters for fuel cell hybrid system applications. Energy Proc 2012;20:301–10.

[8] Solero L, Lidozzi A. Design of multiple-input power converter for hybrid vehicles. IEEE Trans Power Electron 2005;20(5):1007–16.

[9] Marchesoni M, Vacca C. New dc–dc converter for energy storage system interfacing in fuel cell hybrid electric vehicles. IEEE Trans Power Electron 2007;22(1):301–8.

[10] Qian Z, Abdel-rahman O. Modeling and control of three-port DC/DC converter interface for satellite applications. IEEE Trans Power Electron 2010;25(3):637–49.

[11] Nie Z, Bekiarov B, Emadi A. An on-line UPS system with power factor correction and electric isolation using BIFRED converter. IEEE Ind Electron Conf 2003;1:361–6.

[12] Nielsen HR, Andersen MAE, Zhang Z, Thomsen OC. Dual-input isolated full-bridge boost dc–dc converter based on the distributed transformers. J IET Power Electron 2012;5(7):1074–83.

[13] Zhang Z, Thomsen OC, Andersen MAE. Modeling and control of a dual-input isolated full-bridge boost converter. In: Proceedings of the Asia international model simulation conference; 2012. pp. 2017–2023.

[14] Chen Y, Liu Y, Lin S. Double-input PWM dc/dc converter for high/low voltage sources. In: Procedings of the telecom energy conference; 2003. pp. 27–32.

[15] Yalamanchili KP, Ferdowsi M. Review of multiple input dc–dc converters for electric and hybrid vehicles. In: Proceedings of the IEEE vehicle power propulsion conference; 2005. pp. 552–555.

[16] Chen Y, Liu Y, Lin S. Double-input PWM dc/dc converter for high-/low-voltage sources. IEEE Trans Ind Electron 2006;53(5):1538–45.

[17] Dobbs BG, Chapman PL. A multiple-input dc–dc converter topology. IEEE Power Electron Lett 2003;99(1):6–9.

[18] Khaligh A. A multiple-input dc–dc converter topology. IEEE Trans Power Electron 2009;24(3):862–8.

[19] Marchesoni M, Vacca C. New dc–dc converter for energy storage system interfacing in fuel cell hybrid electric vehicles. IEEE Trans Power Electron 2007;22(1):301–8.

[20] Wai R, Lin C, Liaw J, Chang Y. Newly designed ZVS multi-input converter. IEEE Trans Ind Electron 2011;58(2):555–66.

[21] Wai R, Lin C, Chen B. High-efficiency dc–dc converter with two input power sources. IEEE Trans Power Electron 2012;27(4):1862–75.

[22] Lee D, Lee M, Hyun D, Choy I. New zero-current-transition PWM dc/dc converters without current stress. IEEE Trans Power Electron 2003;18(1):95–104.

[23] Yalamanchili KP, Ferdowsi M, Corzine K. New double input dc–dc converters for automotive applications. In: Proceedings of the IEEE vehicle power propulsion conference; 2006. pp. 1–6.

[24] Gavriş M, Cornea O, Muntean N. Multiple input dc–dc topologies in renewable energy systems – a general review. In: Proceedings of the IEEE exploitation of renewable energy sources symposium; 2011. pp. 123–128.

[25] Liu Y, Chen Y. A systematic approach to synthesizing multi-input dc–dc converters. IEEE Trans Power Electron 2009;24(1):116–27.

[26] Kumar L, Jain S. A multiple source dc/dc converter topology. J Electr Power Energy Syst 2013;51:278–91.

[27] Kwasinski A. Identification of feasible topologies for multiple-input dc–dc converters. IEEE Trans Power Electron 2009;24(3):856–61.

[28] Li Y, Ruan X, Yang D, Liu F, Tse CK. Synthesis of multiple-input dc/dc converters. IEEE Trans Power Electron 2010;25(9):2372–85.

[29] Muntean N, Gavris M, Cornea O. Dual input hybrid dc–dc converters. In: Proceedings of the IEEE International computer as a tool conference; 2011. pp. 1–4.

[30] Cornea O, Muntean N, Teodorescu R, Gavris ML. Dual input hybrid buck LC converter for a mixed wind and PV array generation system. In: Proceedings of the international power electronics motion control conference; 2012. pp. 22-1–22-6.

[31] Gavris M, Cornea O, Muntean N. Dual input hybrid buck LC converter. Int Symposium Power Electron Drives Autom Motion 2012;2:309–14.

[32] Kumaravel S, Ashok S. Design and analysis of multiple input power conditioner for SolarPV/Wind hybrid energy system. In: Proceedings of the IEEE region 10 conference; 2011. pp. 883–887.

[33] Bonizzonil E, Borghettil F, Malcovati P. A 200 mA 930/O peak efficiency single-inductor dual-output dc–dc buck converter. In: Proceedings of the IEEE international solid-state circuits conference; 2007. pp. 526–528.

[34] Lin K, Huang C, Chen D, Liu KH, Sido SD. Modeling and design of feedback loops for a buck converter. In: Proceedings of the IEEE power electron specialists conference; 2008. pp. 3389–3395.

[35] Belloni M, Bonizzoni E, Maloberti F. On the design of single-inductor double-output dc–dc buck, boost and buck–boost converters. In: Proceedings of the IEEE electronics, circuits and systems conference; 2008. pp. 626–629.

[36] Ray O, Josyula AP, Mishra S, Joshi A. Integrated dual-output converter. IEEE Trans Ind Electron 2014. http://dx.doi.org/10.1109/TIE.2014.2327599 (in press).

[37] Kwon D, Rincón-mora GA. Single-inductor–multiple-output switching dc–dc converters. IEEE Trans Circuits Syst 2009;56(8):614–8.

[38] Rojas-gonz MA, Edgar S. An integrated dual-output buck converter based on sliding mode control. In: Proceedings of the IEEE third Latin American symposium on circuits and systems; 2012. pp. 1–4.

[39] Xu W, Li Y, Gong X, Hong Z, Killat D, Sido AS. A dual-mode single-inductor dual-output switching converter with small ripple. IEEE Trans Power Electron 2010;25(3):614–23.

[40] Bahrani B, Dasika JD, Saeedifard M, Karimi A, Rufer A. Multivariable control of single-inductor. IEEE Trans Power Electron 2013;99:1103–8.

[41] Belloni M, Bonizzoni E, Maloberti F. On the design of single-inductor multiple-output dc–dc buck converters. In: Proceedings of the IEEE circuits system symposium; 2008. pp. 3049–3052.

[42] dos Santos EC. Dual-output dc–dc buck converters with bidirectional and unidirectional characteristics. IET J.Power Electron 2013;6(5):999–1009.

[43] Santos EC. Single-input dual-output dc–dc buck converter. IEEE Ind Electron Symp 2012;3:496–502.

[44] Jafari M, Hunter G, Zhu JG. A new topology of multi-input multi-output buck–boost dc–dc converter for microgrid applications. In: Proceedings of the IEEE international power energy conference; 2012. pp. 2–5.

[45] Zhoul Z., Wul H., Xingl V.. A non-isolated three-port converter for stand-alone renewable power system. In: Proceedings of the IEEE Industrial Electronics Society Conference; 2012. 3(c). pp. 3352–3357.

[46] Wu H, Xing Y, Xia Y, Sun K. A family of non-isolated three-port converters for stand-alone renewable power system. In: Proceedings of the IEEE Industrial Electronics Society Conference; 2011. 3. pp. 1030–1035.

[47] Ding S, Wu H, Xing Y, Fang Y, Ma X. Topology and control of a family of non-isolated three-port dc–dc converters with a bidirectional cell. In: Proceedings of the IEEE applied power electron conference; 2013. pp. 1089–1094.

[48] Wu H, Zhang J, Xing Y. A family of multi-port buck-boost converters based on dc-link-inductors (DLIs). IEEE Trans Power Electron 2014. http://dx.doi.org/10.1109/TPEL.2014.2307883 (in press).

[49] Wu H, Sun K, Ding S, Xing Y. Topology derivation of nonisolated three-port dc–dc converters from DIC and DOC. IEEE Trans Power Electron 2013;28(7):3297–307.

[50] Hosseini S.H., Haghighian S.K., Danyali S., H. Aghazadeh. Multi-input dc boost converter supplied by a hybrid PV/Wind turbine power systems for street lighting application connected to the grid. In: Proceedings of the University Power Engineering Conference; 2012. pp. 1–6.

[51] Nejabatkhah F, Danyali S, Hosseini SH, Sabahi M, Niapour SM. Modeling and control of a new three-input dc–dc boost converter for hybrid PV/FC/battery power system. IEEE Trans Power Electron 2012;27(5):2309–24.

[52] Nahavandi A, Tarafdar Hagh M, Sharifian MB, Danyali S. A nonisolated multi-input multi-output dc–dc boost converter for electric vehicle applications. IEEE Trans Power Electron 2014. http://dx.doi.org/10.1109/TPEL.2014.2325830 (in press).

[53] Shao H, Li X, Tsui C-Y, Ki W-H. A novel single-inductor dual-input dual-output dc–dc converter with pwm control for solar energy harvesting system. IEEE Trans Very Large Scale Integr 2014. http://dx.doi.org/10.1109/TVLSI.2013.2278785 (in press).

[54] Xiao W, Ozog N, Dunford WG. Topology study of photovoltaic interface for maximum power point tracking. IEEE Trans Power Electron 2007;54(3):1696–1704.

[55] Durán E, Galán J, Andújar JM. Comparative analysis of buck–boost converters used to obtain I–V characteristic curves of photovoltaic modules. In: Proceedings of the IEEE power electron specialists conference; 2008. pp. 2036–2042.

[56] Taghvaee MH, Radzi MAM, Moosavain SM, Hizam H, Hamiruce Marhaban M. A current and future study on non-isolated dc–dc converters for photovoltaic applications. J Renew Sustain Energy Rev 2013;17:216–27.

[57] Chiang SJ. Modeling and control of PV charger system with SEPIC converter. IEEE Trans Ind Electron 2009;56(11):4344–53.

[58] Choung SH, Kwasinski A. Multiple-input dc–dc converter topologies comparison. In: Proceedings of the IEEE industrial electronics conference; 2008. pp. 2359–2364.

[59] Poshtkouhi S, Palaniappan V, Fard M, Trescases O. A general approach for quantifying the benefit of distributed power electronics for fine grained MPPT in photovoltaic applications using 3-D modeling. IEEE Trans Power Electron 2012;27(11):4656–66.

[60] Mohan N. First-course-on-power-electronics-and-drives. M.N., USA: MNPRE; 2003.

[61] Wangl J, Reinhard M, Peng ZF, Qian Z. Design guideline of the isolated dc–dc converter in green power applications. In: Proceedings of the IEEE power electron and motion control conference; 2004. 3. pp. 1756–1761.

[62] Tao H, Kotsopoulos A, Duarte JL, Hendrix MAM. Family of multiport bidirectional dc–dc converters. In: Proceedings of the IEEE electronics power applications conference; 2006. pp. 451–458.

[63] Duarte JL, Hendrix MAM. Multiport converters for hybrid power sources. In: Proceedings of the IEEE power electronics specialists conference; 2008. pp. 3412–3418.

[64] Chen Y, Liu Y, Wu F, Wu T. Multi-input dc/dc converter based on the flux additivity. In: Proceedings of the IEEE Industry Applications Conference; 2001. pp. 1866–1873.

[65] Chen Y, Liu Y, Wu F. Multi-input dc/dc converter based on the multiwinding transformer for renewable energy applications. IEEE Trans Ind Appl 2002;38(4):1096–104.

[66] Chiu H-J, Huang H-M, Lin L-W, Tseng M-H. A multiple-input dc–dc converter for renewable energy systems. In: Proceedings of the IEEE industrial technology conference; 2005. pp. 1304–1308.

[67] Yang D, Ruan X, Li Y, Liu F. Multiple-input full bridge dc–dc converter. In: Proceedings of the IEEE energy conversion congress and exposition; 2009. 4(29). pp. 2881–2888.

[68] Wai R, Lin C, Chang Y. High step-up bidirectional isolated converter with two input power sources. IEEE Trans Ind Electron 2009;56(7):2629–43.

[69] Suetomi M, Matsuo H, Nakashima R, Hamaguchi R, Isizuka Y, Lin W. A novel multi-input dc–dc converter with high power efficiency. In: Proceedings of the IEEE telecom energy conference; 2011. pp. 1–5.

[70] Yu S-Y, Kwasinski A. Multiple-input soft-switching converters in renewable energy applications. In: Proceedings of the IEEE Energy Conversion Congress and Exposition; 2012. pp. 1711–1718.

[71] Zhang Z, Thomsen OC, Andersen MAE, Nielsen HR. A novel dual-input isolated current-fed dc–dc converter for renewable energy system. In: Proceedings of the IEEE applied power electronics conference and exposition; 2011. pp. 1494–1501.

[72] Nielsen HR, Andersen MAE, Zhang Z, Thomsen OC. Dual-input isolated full-bridge boost dc–dc converter based on the distributed transformers. J IET Power Electron 2012;5(7):1074–83.

[73] Wu H, Sun K, Chen R, Hu H. Full-bridge three-port converters with wide input voltage range for renewable power systems. IEEE Trans Power Electron 2012;27(9):3965–74.

[74] Ding Z, Yang C, Zhang Z, Wang C, Xie S. A novel soft-switching multiport bidirectional dc–dc converter for hybrid energy storage system. IEEE Trans Power Electron 2014;29(4):1595–609.

[75] Liu D, Li H. A ZVS bi-directional dc–dc converter for multiple energy storage elements. IEEE Trans Power Electron 2006;21(5):1513–7.

[76] Liu D, Li H, Marlino LD. Design of a 6 kW multiple-input bi-directional dc-dc converter with decoupled current sharing control for hybrid energy storage elements. In: Proceedings of the IEEE twenty second applied power electronics conference; 2007. pp. 509–513.

[77] Ma X, Wu H, Yue X. PWM and phase-shifted control method for isolated asymmetric half-bridge bi-directional converter. In: Proceedings of the IEEE power electronics specialists conference; 2008. pp. 3665–3670.

[78] Tao H, Kotsopoulos A, Duarte JL, Hendrix MAM. Triple-half-bridge bidirectional converter controlled by phase shift and PWM. In: Proceedings of the IEEE twenty-first applied power electronics conference and exposition; 2006. pp. 1256–1262.

[79] Liu S, Zhang X, Guo H, Xie J. Multiport dc/dc converter for stand-alone photovoltaic lighting system with battery storage. In: Proceedings of the IEEE international electrical and control engineering conference; 2010. pp. 3894–3897.

[80] Tao H, Duarte JL, Hendrix MAM. Three-port triple-half-bridge bidirectional converter with zero-voltage switching. IEEE Trans Power Electron 2008;23(2):782–92.

[81] Xie J, Zhang X, Zhang C, Wang C, Liu S. Design of multiple-input dc–dc converter control system for fuel cell electrical vehicle. In: Proceedings of the IEEE Energy and Environment Technology Conference 2009. pp. 123–126.

[82] Al-Atrash H, Reese J, Batarseh I. Tri-modal half-bridge converter for three-port interface. In: Proceedings of the IEEE power electronics specialists conference; 2007. pp. 1702–1708.

[83] Qian Z, Abdel-Rahman O, Hu H, Batarseh I. An integrated three-port inverter for stand-alone pv applications. In: Proceedings of the IEEE Energy Converion Congress and Exposition; 2010. pp. 1471–1478.

[84] Qian Z, Abdel-Rahman O, Hu H, Batarseh I. Multi-channel three-port dc/dc converters as maximum power tracker, battery charger and bus regulator. In: Proceedings of the IEEE twenty-fifth applied power electronics conference and exposition; 2010. pp. 2073–2079.

[85] Wu H, Xing Y, Zhang J, Sun K. A three-port half-bridge converter with synchronous rectification for renewable energy application. In: Proceedings of the IEEE Energy Conversion Congress and Exposition; 2011. pp. 3343–3349.

[86] Zhang Z, Thomsen OC, Andersen MAE. Dual-input soft-switched dc–dc converter with isolated current-fed half-bridge and voltage-fed full-bridge

for fuel cell or photovoltaic systems. In: Proceedings of the IEEE twenty-eighth applied power electronics conference exposition; 2013. pp. 2042–2047.

[87] Li W, He Y, He X, Sun Y. Series asymmetrical half-bridge converters with voltage autobalance for high input-voltage applications. IEEE Trans Power Electron 2013;28(8):3665–74.

[88] Samavatian V, Bathaee SM, Fereidunian.A. Half-bridge current-fed multi-resonant bidirectional three-port dc dc converter for flexible distributed generations. Power Electronics and Drive System Technologies Conference; 2014. pp. 172–176.